Principles of Galaxy Structure

Balance between gravity and…

- Angular momentum (rotation)
- Random motions (“dynamical pressure”)

Disks and spheroids will typically obey straightforward scaling relations, controlled by fairly simple dynamics

1

Principles of Galaxy Structure

Mix of nature vs nurture

- Properties of initial overdensity + statistical properties of surrounding density field set mass, angular momentum, time of collapse+accretion, to first order (for a given dark matter model)
- Internal evolution (instabilities), specifics of mergers, feedback from SNe+AGN, further shape structure.

X

Principles of Galaxy Structure

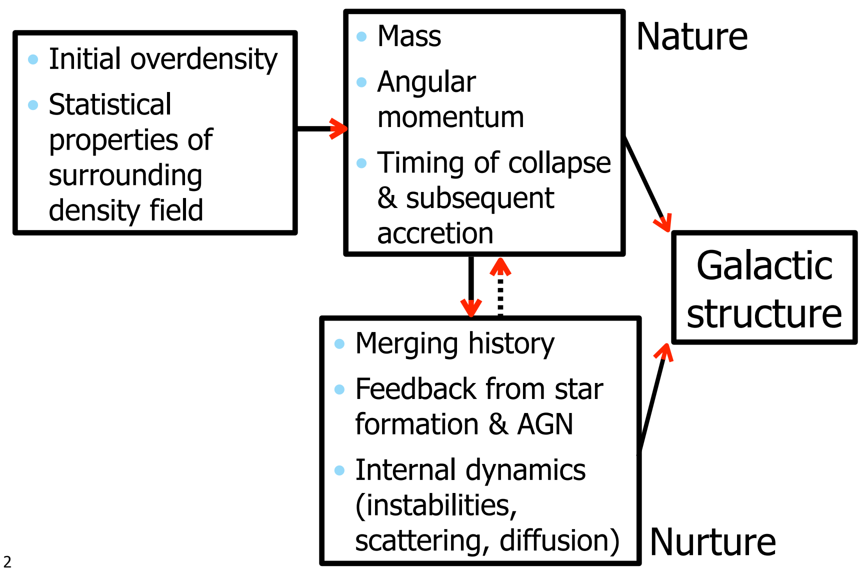

2

Today

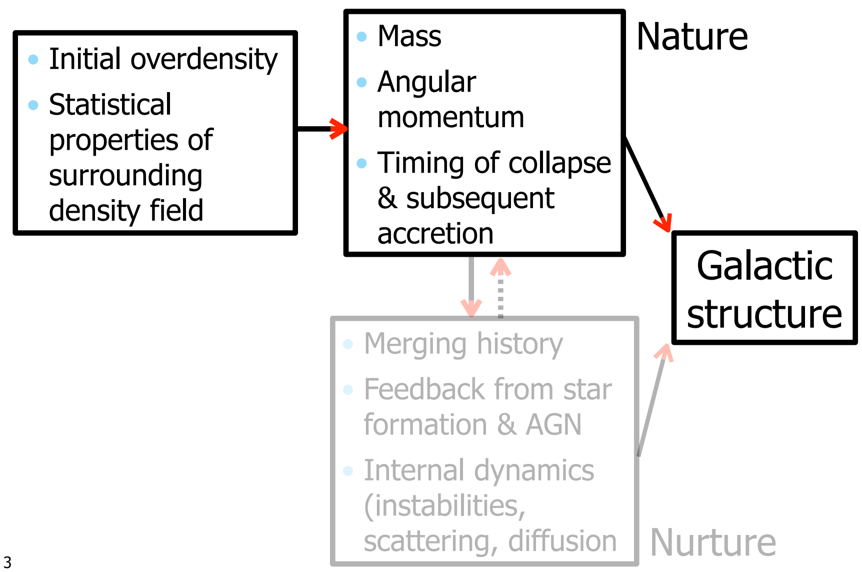

3

Some simple but useful scalings

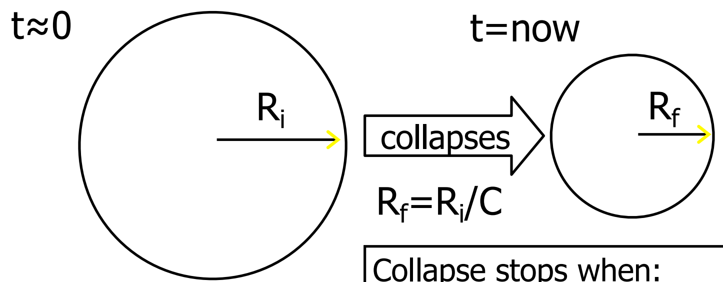

Mass M ~ $\rho(t\approx0)R_i^3$

Density of the early universe, which can be assumed to be fairly uniform

Collapse stops when:

1. Virialization occurs (if dissipationless collapse, like for dark matter or stars)
2. Centripital force (set by angular momentum) balances inwards pull of gravity (if dissipational, like for gas)

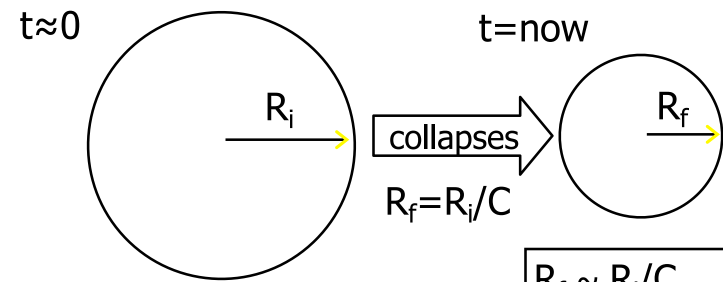

Mass M ~ $\rho(t\approx0)R_i^3$

Density of the early universe, which can be assumed to be fairly uniform and close to ρ_{crit}

$R_f \sim R_i/C$
$\sim (M/\rho)^{1/3} / C$
$\sim M^{1/3} (C^{-1} \rho^{-1/3})$

So size increases as $M^{1/3}$

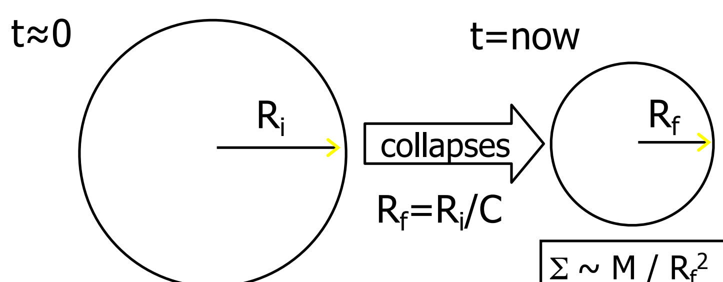

Mass M ~ $\rho(t\approx0)R_i^3$

Density of the early universe, which can be assumed to be fairly uniform

$\Sigma \sim M / R_f^2$
$\sim C^2 M / R_i^2$
$\sim C^2 M / (M/\rho)^{2/3}$
$\sim M^{1/3} (C^2 \rho^{2/3})$

So surface density and size both increase as $M^{1/3}$

Broadly:

$R_f \sim R_i/C$
$\sim (M/\rho)^{1/3} / C$
$\sim M^{1/3} (C^{-1} \rho^{-1/3})$

$\Sigma \sim M / R_f^2$
$\sim C^2 M / R_i^2$
$\sim C^2 M / (M/\rho)^{2/3}$
$\sim M^{1/3} (C^2 \rho^{2/3})$

- At same collapse factor C, the radius R and surface density Σ increase like $M^{1/3}$
- Within similar formation pathways, more massive galaxies will tend to be physically larger and higher surface density

Broadly:

$R_f \sim R_i/C$
$\sim (M/\rho)^{1/3} / C$
$\sim M^{1/3} (C^{-1} \rho^{-1/3})$

$\Sigma \sim M / R_f^2$
$\sim C^2 M / R_i^2$
$\sim C^2 M / (M/\rho)^{2/3}$
$\sim M^{1/3} (C^2 \rho^{2/3})$

- At same mass, larger collapse factors lead R to decrease and Σ to increase
- Larger collapse factors result from:
  - Less initial spin, when the collapse is halted by angular momentum
  - More dissipation, when collapse is halted by dynamical pressure (velocity dispersion)

Broadly:

$R_f \sim R_i/C$
$\sim (M/\rho)^{1/3} / C$
$\sim M^{1/3} (C^{-1} \rho^{-1/3})$

$\Sigma \sim M / R_f^2$
$\sim C^2 M / R_i^2$
$\sim C^2 M / (M/\rho)^{2/3}$
$\sim M^{1/3} (C^2 \rho^{2/3})$

- At the same mass and formation pathway, galaxies that collapsed from higher characteristic initial densities will be denser and more compact.
- Initial density dependence can potentially imprint a timing+environmental bias (Larger overdensities collapse faster, starts denser, forms earlier)

Now look at:

Global Trends in Size, Surface Brightness & Magnitude

Scale Lengths

Surface brightnesses

Size vs Surface Brightness

Basic scaling relations with mass

1. Faint galaxies are smaller

Massive Ellipticals: $r_{50} \sim 10$ kpc

Massive Spirals: $r_{50} \sim$ 5-8 kpc

Dwarfs: $r_{50} \sim 1$ kpc

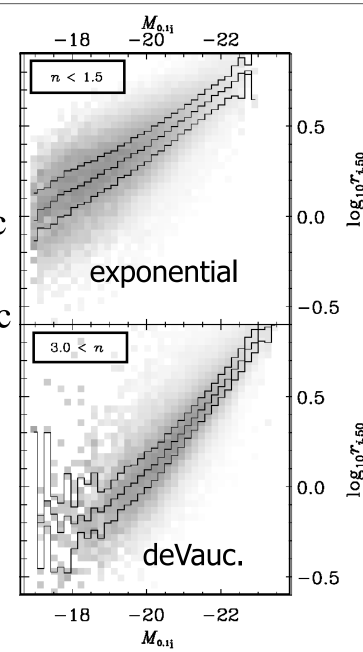

Blanton et al 2003 **(r_{50} in h^{-1} kpc)**
This analysis corrects for relative numbers. At each absolute magnitude, the vertical grayscale indicates the relative distribution of sizes.

Sizes of Large Spiral Disks

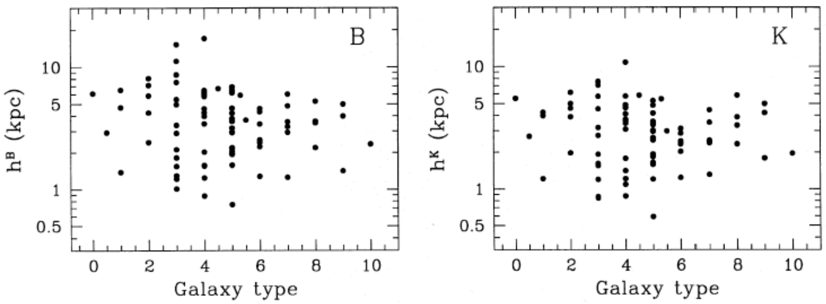

Milky Way has h_r ~ 2.5-3.5 kpc

Note: this is just one particular sample, and is not necessarily representative of the entire disk galaxy population!

(Warning: H_0 varies in older papers!)

de Jong 1996

Sizes of Gas Rich Dwarf Galaxies

Again, not representative of the whole population -- just an indication of the general sizes you'd find.

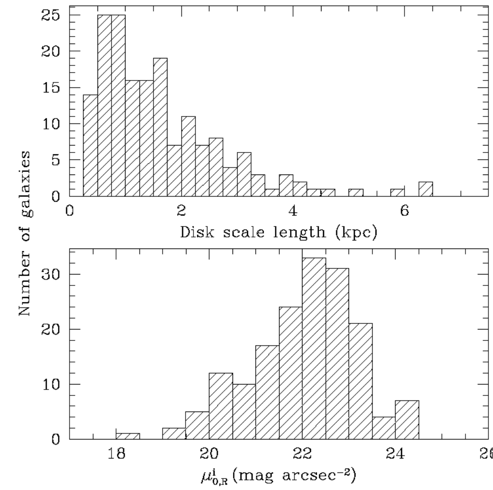

Fig. 15. The distribution of scale lengths (top panel) and of inclination corrected central surface brightnesses for the galaxies in our sample.

Swaters & Balcells 2002

2. Fainter Galaxies have lower surface brightnesses

But, the magnitude-surface brightness relation distribution is wide.

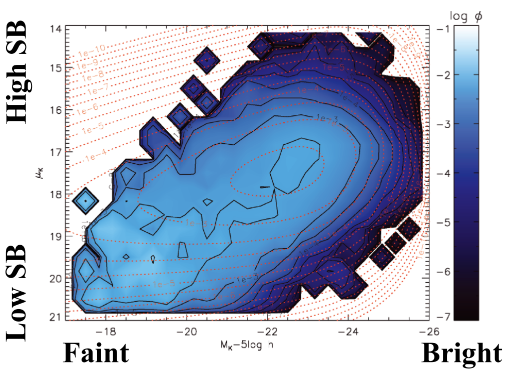

Figure 11. BBD for the full sample in K-band absolute magnitude and absolute effective surface brightness. Shaded regions and solid black contours show the space density, ϕ, as in Fig. 10. The best-fitting Chołoniewski function, estimated using $M_K - 5\log h < -20$ and $\mu_{e,abs} < 19$, is shown by the red dotted contours. Parameters of the fit are $M^* - 5\log h = -22.96$ mag, $\alpha = -0.38$, $\phi^* = 0.0201\,h^3\,\mathrm{Mpc}^{-3}$, $\mu^*_{e,abs} = 17.36$ mag arcsec^{-2}, $\sigma_{\mu_{e,abs}} = 0.672$ mag arcsec^{-2} and $\beta = 0.188$.

Watch selection effects!

("BBD"=bivariate brightness distribution)

Smith et al 2009

Broad trend does agree with expected scaling

Surface density and size both increase as $M^{1/3}$

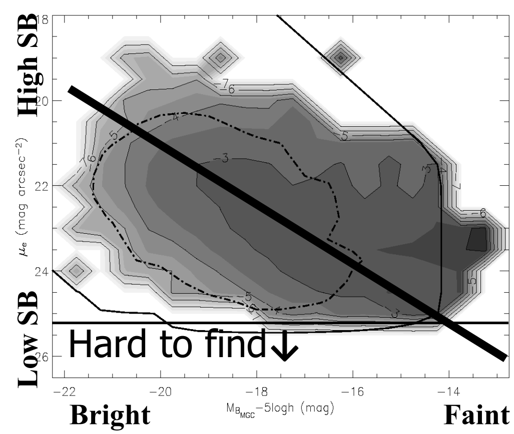

Figure 12. The final space density or bivariate brightness distribution of galaxies shown as both a greyscale image and contours on logarithmic scales in units of h^3 Mpc^{-3} mag^{-1} (mag arcsec^{-2})$^{-1}$. The contour spacing is 1 dex in ϕ with the greyscale at 0.5 dex intervals. The thick solid line denotes the selection boundary defined as the BBD region where at least 100 galaxies could have been detected and is equivalent to an effective volume limit of 1800h^{-3}Mpc^3. The thick dashed line encompasses the region within which the statistical error is smaller than 25 per cent.

Driver et al 2005

Luminosity vs Surface Brightness

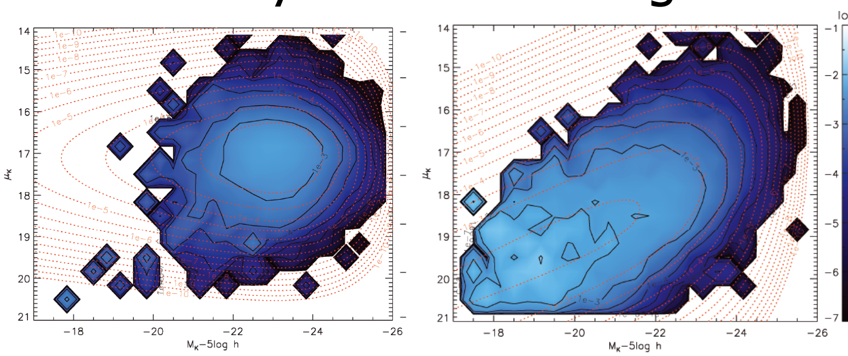

Red Galaxies

u-r > 2.35

Blue Galaxies

u-r < 2.35

Smith et al 2009

Luminous, high surface brightness galaxies tend to be quiescent

Fainter Galaxies have lower surface brightnesses

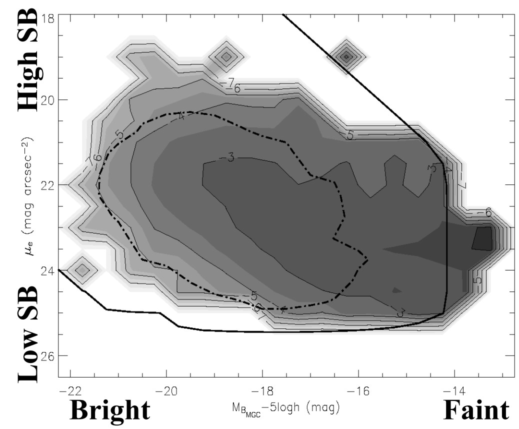

Figure 12. The final space density or bivariate brightness distribution of galaxies shown as both a greyscale image and contours on logarithmic scales in units of h^3 Mpc^{-3} mag^{-1} (mag arcsec^{-2})$^{-1}$. The contour spacing is 1 dex in ϕ with the greyscale at 0.5 dex intervals. The thick solid line denotes the selection boundary defined as the BBD region where at least 100 galaxies could have been detected and is equivalent to an effective volume limit of $1800h^{-3}$Mpc^3. The thick dashed line encompasses the region within which the statistical error is smaller than 25 per cent.

But, the magnitude-surface brightness relation distribution is wide.

Watch selection effects!

("BBD"=bivariate brightness distribution)

Driver et al 2005

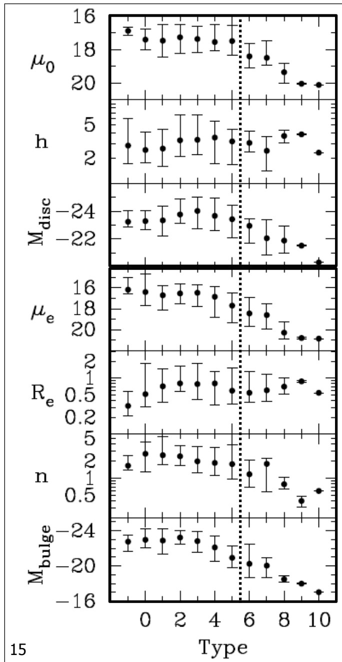

Surface Brightness vs Mass trend imprints morphologically: μ tends to fall for late-type galaxies (T>Sc)

A manifestation of the fact that later types are fainter, and fainter galaxies have lower surface brightness. Note also that Sa-Sc's are similar.

Graham & Worley 2008

Figure 3. Standard $\boxed{K\text{-band}}$ disc and bulge structural properties as a function of galaxy Type. For the disc, μ_0, h and $M_{\rm disc}$ are the central surface brightness, scale-length and absolute magnitude. For the bulge, μ_e, R_e, n and $M_{\rm bulge}$ are the effective surface brightness, effective half-light radius, Sérsic index and absolute magnitude. The data have been taken from Table 3, except for the bulge magnitudes which have been taken from Table 4. For each T-Type, the median is marked with a circle and the 'error bars' denote the 16 and 84 per cent quartiles of the full distribution, rather than uncertainties on the median value.

3. Disk Scale Length vs Surface Brightness

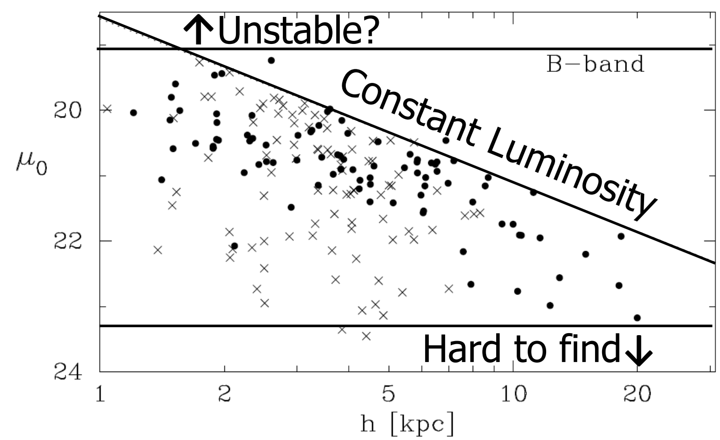

Figure 9. B-band. Central disc surface brightness (corrected using equation 1) versus disc scalelength (corrected using equation 2). Rather than a Freeman (1970) law of constant surface brightness, an upper bright envelope, which has been seen before (e.g. Graham 2001b and references therein), is evident. The empirically-fitted dotted line in this diagram is such that $\mu_{0,bright} = 18.6 + 2.5\log h$. Galaxy types Sbc ($T = 4$) and earlier are denoted by circles, while later galaxy types are denoted by crosses. The noticeably broader distribution for the late-type disc galaxies has also been noted before (Graham & de Blok 2001).

 Graham & Worley 2008

Revisiting Structural Parameters

Data from a wide variety of sources.
(Don't attatch meaning to the relative density of points)

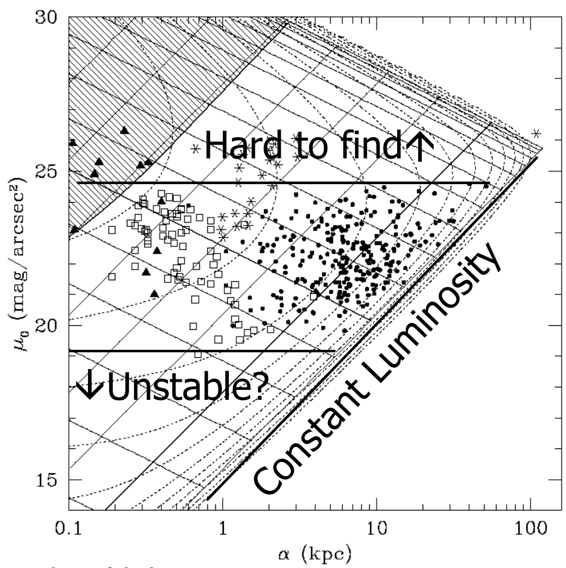

h_r used to be called α in the old days…

Dalcanton et al 1997

Dissipational Collapse, halted by angular momentum

Existence and slope of Luminosity-Surface brightness relationship, and diagonal upper limit in h_r vs μ_0 consistent with dissipational collapse halted by angular momentum

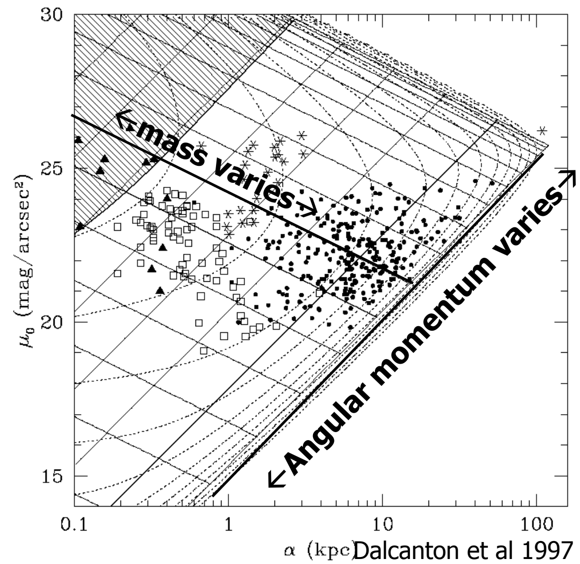

Dalcanton et al 1997

Broadly:

$$R_f \sim R_i/C \sim (M/\rho)^{1/3} / C \sim M^{1/3} (C^{-1} \rho^{-1/3})$$

$$\Sigma \sim M / R_f^2 \sim C^2 M / R_i^2 \sim C^2 M / (M/\rho)^{2/3} \sim M^{1/3} (C^2 \rho^{2/3})$$

But

This is far from the whole picture.
Internal evolution?, Feedback?, etc

These may have their own internal scalings with mass, and some self-regulation that keeps overall scaling intact.

For example, at high disk surface densities, you make bulges instead.

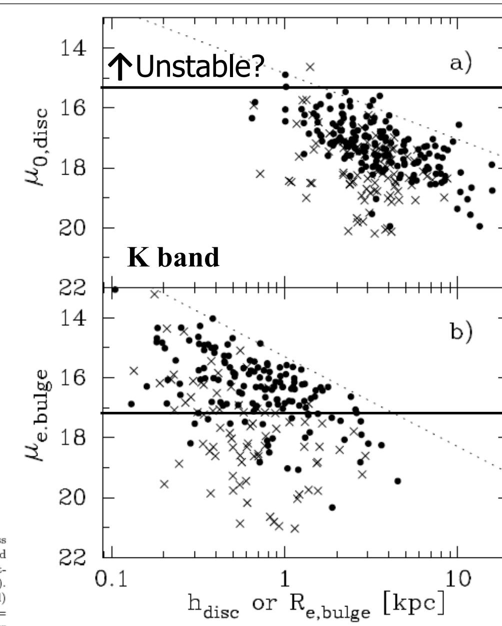

Horizontal line is at same μ_e for n=1

Figure 8. K-band. Top panel: Central disc surface brightness (corrected using equation 1) versus disc scalelength h (corrected using equation 2). Bottom panel: Bulge effective surface brightness (observed) versus the bulge effective radius R_e (observed). The upper bright envelope is traced here with the (empirical) lines $\mu_{0,\mathrm{bright}} = 14.85 + 2.2 \log h$ (panel a) and $\mu_{e,\mathrm{bright}} = 15.3 + 3.0 \log R_e$ (panel b). Galaxy types Sbc ($T = 4$) and earlier are denoted by the circles, while later galaxy types are denoted by the crosses.

Graham & Worley 2008

What constrols vertical surface brightness distributions?

Vertical Structure of Disks

Exponential at large scale heights

Different possible structures at midplane

Profile set by balance of gravity and dynamical pressure

Dynamical pressure set by “vertical heating”

Depends on galaxy mass and/or T-type

Obviously, dust is a problem

- Near-IR ideal
- R or I-band sometimes used for better FOV and/or sensitivity

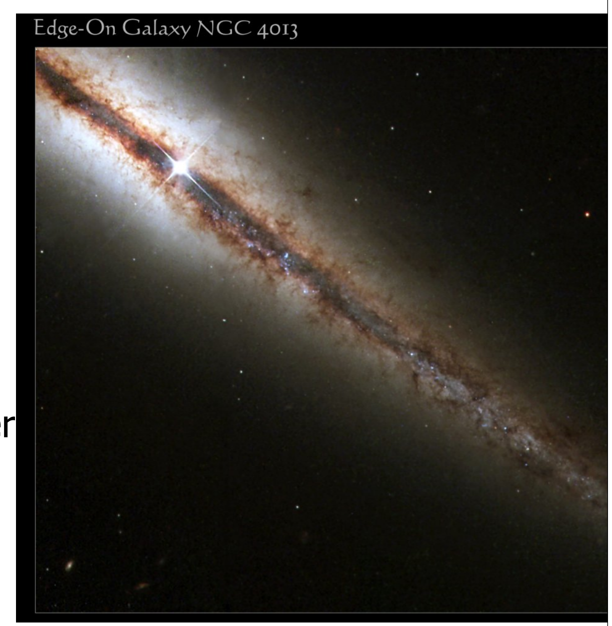

Vertical light distributions of disks:

Edge-on galaxies in the I-band.

Generally rounder at low light levels, probably due to analogs of MW thick disks.

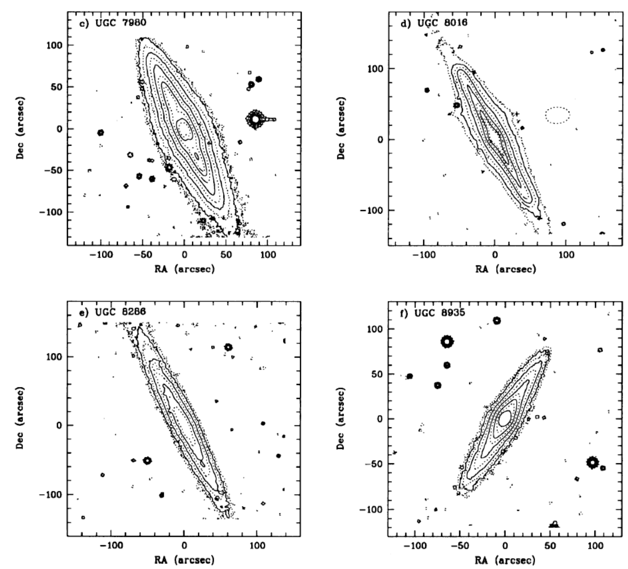

Falls off with z as straight line in μ

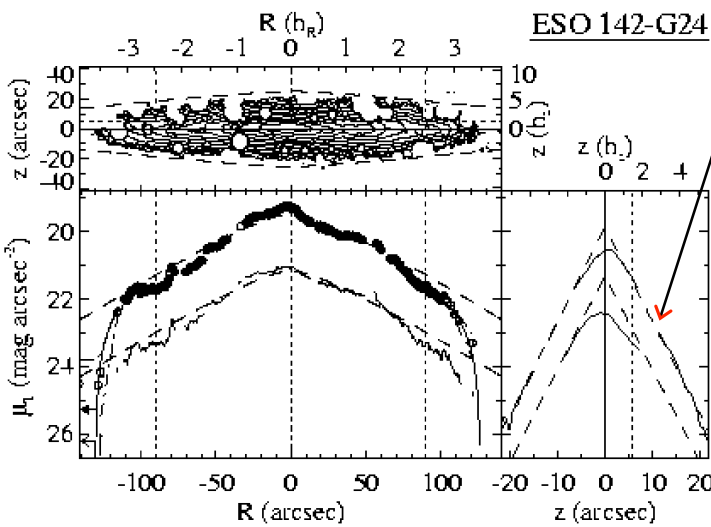

Kregel et al 2002

Fitting formula for vertical surface brightness

Isothermal, self-gravitating sheet (Spitzer 1942)

$$L(z) = L_0 \, \mathrm{sech}^2(z/z_0)$$

Exponential

$$L(z) = L_0 \exp(-z/h_z)$$

Generalized (van der Kruit 1988) [$z_0 \approx 2h_z$]

$$L(z) = 2^{-2/n} L_0 \, \mathrm{sech}^{2/n}(nz/2z_0)$$

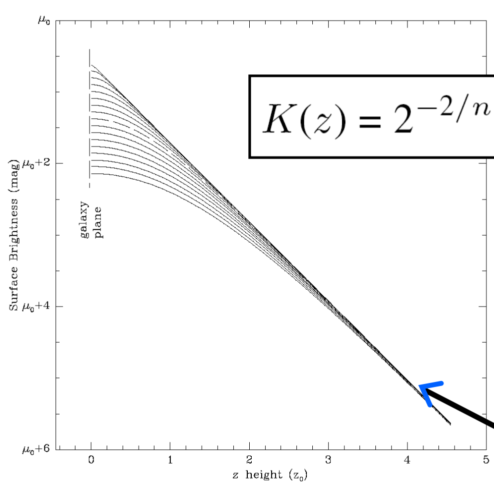

$$K(z) = 2^{-2/n} K_0 \, \mathrm{sech}^{2/n}(nz/2z_0)$$

Isothermal if n=1

Exponential if n=∞

They all look the same at large z

Fig. 4. The family of density (luminosity) laws (6) with the isothermal ($2/n$ = 2.0) and the exponential ($2/n$ = 0.0) distributions as the two extremes. The difference in $2/n$ between two successive model distributions is 0.125; for clarity, the sech(z) model distribution ($2/n$ = 1.0) is shown as the dashed profile (μ_0 is the central surface brightness).

de Grijs et al 1997

The exponential distribution is typically adopted however, since differences are only pronounced near the midplane:

Luminosity density in space:

$$L(R, z) = L_0 \; e^{-R/h_\mathrm{R}} e^{-z/h_\mathrm{z}}$$

Projected surface brightness, seen edge-on:

$$\boxed{\Sigma_{\rm disc}(R', z) = \Sigma_0\ (R'/h_{\rm R})\ K_1(R'/h_{\rm R})\ e^{-z/h_z}}, \quad (2)$$

where R' is the projected radius along the major axis, $\Sigma_0 = 2h_{\rm R}L_0$ is the projected *edge-on* central surface brightness and K_1 is the modified Bessel function of the first order.

(assumes optically thin disk!) Van der Kruit & Searle 1981

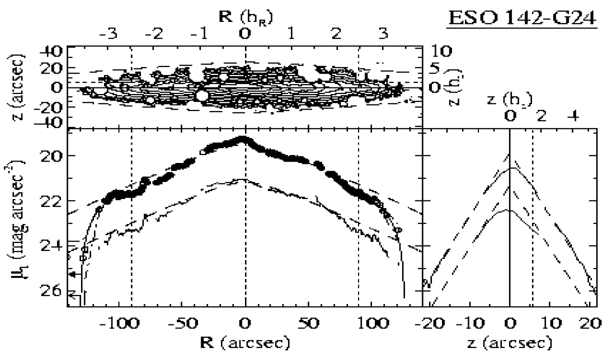

Kregel et al 2002

Scale heights tend to be < 1 kpc

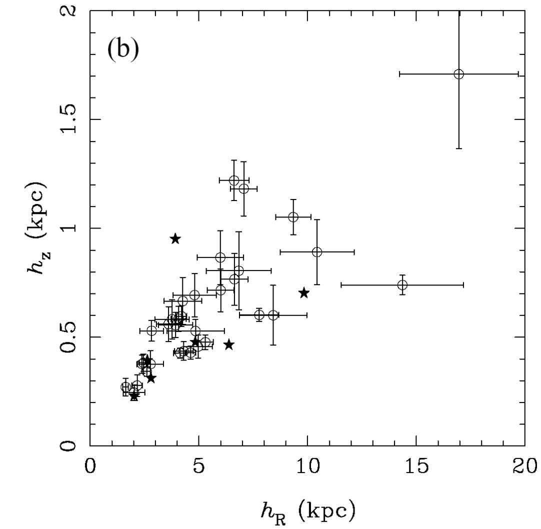

Kregel et al 2002

Lower mass, fainter galaxies tend to be puffier

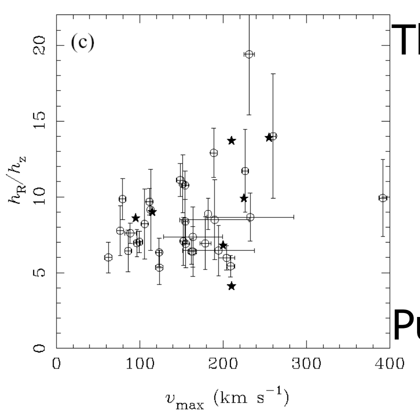

Thin

Puffy

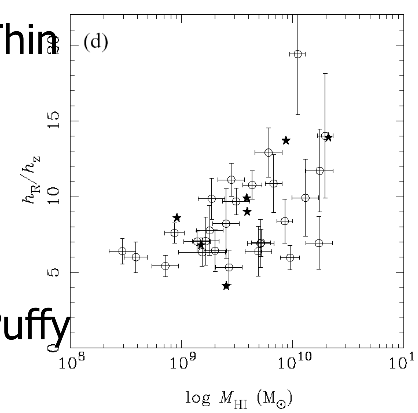

Rotation Speed Gas Mass (HI)

Kregel et al 2002

Contradicts…

Bulge fitting problems, I think…

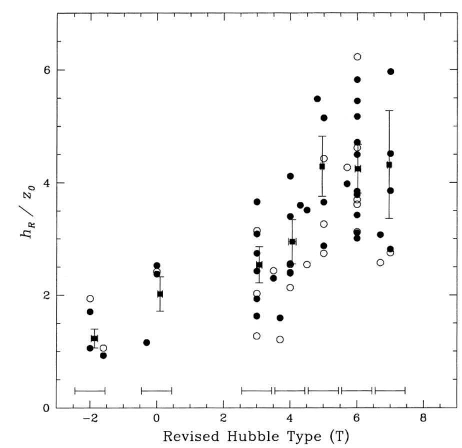

Figure 6. Dependence of the h_R/z_0 ratio on galaxy type for both *I*-band data (filled dots) and *K*-band observations (open circles). The filled squares show the *I*-band ratios averaged over the type bins indicated by the horizontal bars; the errors indicate the standard deviations of the distribution.

de Grijs 1998

Disk flares for early types, but not late-types

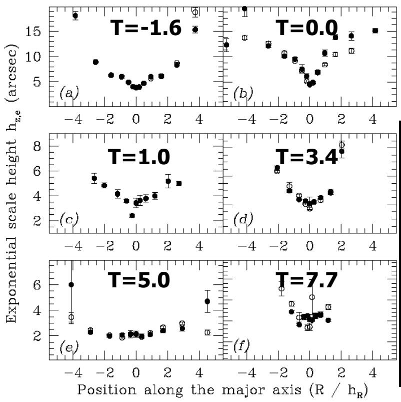

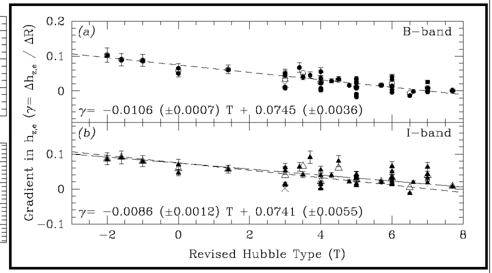

Fig. 1. Examples of the *I*-band scale height behaviour as a function of galactocentric distance for *(a)* ESO 358G-29 (T = −1.6), *(b)* ESO 311G-12 (T = 0.0), *(c)* ESO 315G-20 (T = 1.0), *(d)* ESO 322G-87 (T = 3.4), *(e)* ESO 435G-50 (T = 5.0), and *(f)* ESO 505G-03 (T = 7.7). Open and closed symbols represent data taken on both sides of the galaxy planes.

de Grijs & Peletier 1997

Why you expect the observed vertical structure:

A slab of stars, with total surface density Σ and vertical density profile $\rho(z)$.

Assume that the slab is "self-gravitating"

↓ $F_z = mg_z$

A particle of mass m at z feels a downward force $F_z = mg_z$, where g_z is the gravitational acceleration (or force field).

Via Gauss's Law:

$$\vec{g} = -\nabla \phi$$

↓ $F_z = mg_z$

$$\nabla \cdot \vec{g} = \nabla^2 \phi = -4\pi G \rho$$

So ignoring horizontal forces (that in a real disk would be due to $\Sigma(r)$)

$$\nabla \cdot \vec{g} \approx \frac{dg_z}{dz} = -4\pi G \rho$$

This is an equation which can be solved!

Via Gauss's Law:

$$\frac{dg_z}{dz} = -4\pi G \rho$$

↓ $F_z = mg_z$

Since forces=0 at the midplane:

$$g_z = -4\pi G \int_0^z \rho(z')dz'$$

If the disk is in equilibrium, then something must be balancing the the gravitational pull.

Dynamical Pressure: $\boxed{P_z = \sigma_z^2 \rho}$

(assuming "isothermal" -- i.e. σ_z constant)

Similar to stellar structure eqn's:

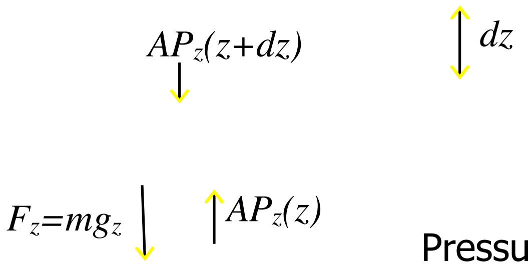

Consider one layer of the slab, with thickness dz, area A, and mass $\rho A dz$

Pressure = Force / Area

$$[P_z(z+dz) - P_z(z)]A = (\rho A dz)g_z$$

Yielding: $$\frac{dP_z}{dz} = \rho g_z$$

Substituting dynamical pressure:

$$\frac{dP_z}{dz} = \rho g_z \longrightarrow \frac{d(\sigma_z^2\rho)}{dz} = \rho g_z$$

$$\sigma_z^2 \frac{1}{\rho}\frac{d\rho}{dz} = g_z \; + \; g_z = -4\pi G \int_0^z \rho(z')dz'$$

A tasty differential equation:

$$\boxed{\frac{d\ln\rho}{dz} = -\frac{4\pi G}{\sigma_z^2}\int_0^z \rho(z')dz'}$$

Substituting dynamical pressure:

$$\frac{dP_z}{dz} = \rho g_z \longrightarrow \frac{d(\sigma_z^2\rho)}{dz} = \rho g_z$$

Rearranging…

$$\sigma_z^2 \frac{1}{\rho}\frac{d\rho}{dz} = g_z$$

Note that this step only worked because the velocity dispersion was constant (I.e. "isothermal"). However, you can model the pressure of more complex distributions as being the sum of the pressure from several populations with different velocity dispersions.

This differential equation:

$$\frac{d\ln\rho}{dz} = -\frac{4\pi G}{\sigma_z^2}\int_0^z \rho(z')dz'$$

Has solutions of the form:

$$\rho(z) = \rho_0 \operatorname{sech}^2\left(\frac{z}{2z_0}\right)$$

Where z_0 is some combination of G, σ_z, & ρ_0

$$\boxed{\frac{d\ln\rho}{dz} = -\frac{4\pi G}{\sigma_z^2}\int_0^z \rho(z')dz'}$$

At large distances above the plane:

$$\int_0^{z\to\infty} \rho(z')dz' \to \frac{\Sigma}{2} \longrightarrow \frac{d\ln\rho}{dz} = -\frac{2\pi G\Sigma}{\sigma_z^2}$$

Which has exponential solutions:

$$\boxed{\rho(z) = \rho_0\, e^{-z/z_0}}$$

Where: $$z_0 = \frac{\sigma_z^2}{2\pi G\Sigma}$$

39 (z_0 is set by the battle between random motions σ_z and self gravity Σ)

Real disks are somewhere between an isothermal and an exponential

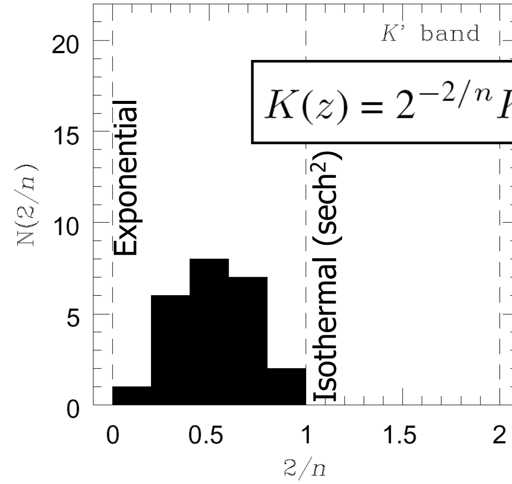

$$\boxed{K(z) = 2^{-2/n} K_0\, \mathrm{sech}^{2/n}(nz/2z_0)}$$

No single vertical velocity dispersion!

40

Why not isothermal?

$$\boxed{\sigma(t) = \sigma_\circ(1+\frac{t}{\tau})^\alpha}$$

Scattering off GMCs & Spiral Arms, and/or accretion

Hanninen & Flynn 2002

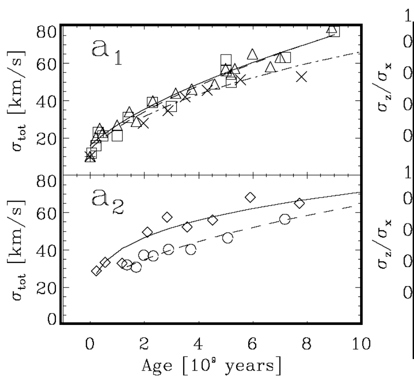

Table 1. Values of the heating index obtained by fitting data in the literature. The first five rows show our fits, and the last two show the author's own reported values. Note that Holmberg (2001) removes the effect of higher velocity thick disc stars when making his (more reliable) estimate of the heating index, whereas we leave them in (in order to estimate the bias they impose). There is a very considerable range in the derived values of α, which far exceeds the reported (internal) error estimates; α is therefore very likely to be dominated by systematic errors in the methods used to estimate stellar ages.

Study	α
R. Wielen (1977)	0.61 ± 0.04
Fuchs et al. (2000)	0.59 ± 0.04
Edvardsson et al.(1993)	0.47 ± 0.002
H. Rocha-Pinto	0.26 ± 0.008
Holmberg (2001) All stars	0.45 ± 0.04
Holmberg (2001) Thick Disc removed	0.33 ± 0.03
Binney et al. (2000)	0.33 ± 0.03

Age [10^9 years]

Figure 1. The observed total stellar velocity dispersion and ratio of velocity dispersions for nearby disc stars, as obtained by different authors. Best fits to the heating laws as parameterised by Eqn. 1 are also shown. Panel (a_1): the solid line is the fit to Fuchs et al. data (triangles), the dashed line is the fit to Wielen's data (squares), and the dot-dashed line is the fit to Edvarsson et al. data (crosses). Panel (a_2): the solid line is the fit to Rocha-Pinto's data (diamonds) and the dashed line is the fit to Holmberg's data (circles). Panels (b_1) and (b_2) show the observed ratios of the vertical to the radial velocity dispersion for the same data sets and using the same symbols.

What might be reasons for the dispersion?

$$\boxed{\rho(z) = \rho_0\, e^{-z/z_0}}$$

$$z_0 = \frac{\sigma_z^2}{2\pi G\Sigma}$$

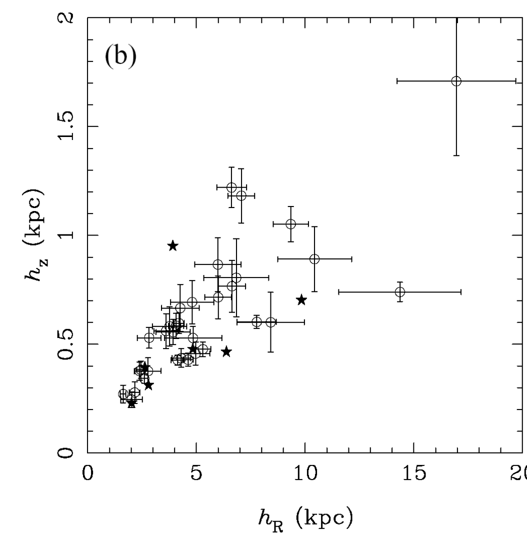

Kregel et al 2002

42

What might be reasons for flaring?

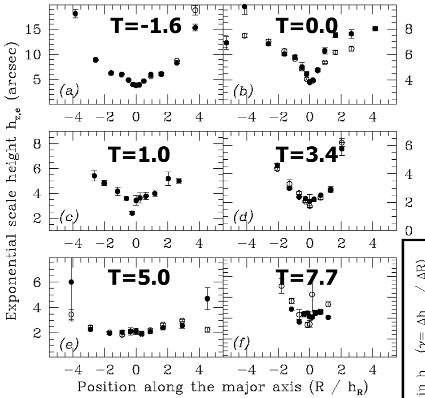

Fig. 1. Examples of the *I*-band scale height behaviour as a func
of galactocentric distance for *(a)* ESO 358G-29 (T = −1.6), *(b)* E
311G-12 (T = 0.0), *(c)* ESO 315G-20 (T = 1.0), *(d)* ESO 322G-87
3.4), *(e)* ESO 435G-50 (T = 5.0), and *(f)* ESO 505G-03 (T = 7.7). C
and closed symbols represent data taken on both sides of the ga
planes.

$$\boxed{\rho(z) = \rho_0\, e^{-z/z_0}}$$

$$z_0 = \frac{\sigma_z^2}{2\pi G \Sigma}$$

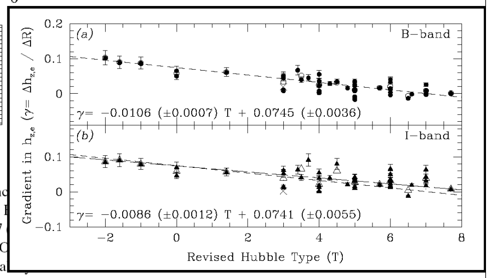

de Grijs & Peletier 1997